

Inhibition of Marburg Virus Budding by Nonneutralizing Antibodies to the Envelope Glycoprotein

Masahiro Kajihara,^a Andrea Marzi,^b Eri Nakayama,^a Takeshi Noda,^c Makoto Kuroda,^a Rashid Manzoor,^a Keita Matsuno,^a Heinz Feldmann,^b Reiko Yoshida,^a Yoshihiro Kawaoka,^{c,d,e,f} and Ayato Takada^{a,g}

Division of Global Epidemiology, Hokkaido University Research Center for Zoonosis Control, Sapporo, Japan^a; Laboratory of Virology, Division of Intramural Research, National Institute of Allergy and Infectious Diseases, National Institutes of Health, Rocky Mountain Laboratories, Hamilton, Montana, USA^b; Division of Virology, Department of Microbiology and Immunology, Institute of Medical Science, University of Tokyo, Tokyo, Japan^c; International Research Center for Infectious Diseases, Institute of Medical Science, University of Tokyo, Tokyo, Japan^d; ERATO Infection-Induced Host Responses Project, Saitama, Japan^e; Department of Pathobiological Science, University of Wisconsin—Madison, Madison, Wisconsin, USA^f; and School of Veterinary Medicine, the University of Zambia, Lusaka, Zambia^g

The envelope glycoprotein (GP) of Marburg virus (MARV) and Ebola virus (EBOV) is responsible for virus entry into host cells and is known as the only target of neutralizing antibodies. While knowledge about EBOV-neutralizing antibodies and the mechanism for the neutralization of infectivity is being accumulated gradually, little is known about antibodies that can efficiently regulate MARV infectivity. Here we show that MARV GP-specific monoclonal antibodies AGP127-8 (IgG1) and MGP72-17 (IgM), which do not inhibit the GP-mediated entry of MARV into host cells, drastically reduced the budding and release of progeny viruses from infected cells. These antibodies similarly inhibited the formation of virus-like particles (VLPs) consisting of GP, the viral matrix protein, and nucleoprotein, whereas the Fab fragment of AGP127-8 showed no inhibitory effect. Morphological analyses revealed that filamentous VLPs were bunched on the surface of VLP-producing cells cultured in the presence of the antibodies. These results demonstrate a novel mechanism of the antibody-mediated inhibition of MARV budding, in which antibodies arrest unformed virus particles on the cell surface. Our data lead to the idea that such antibodies, like classical neutralizing antibodies, contribute to protective immunity against MARV and that the “classical” neutralizing activity is not the only indicator of a protective antibody that may be available for prophylactic and therapeutic use.

Marburg virus (MARV) has a nonsegmented, single-stranded, negative-sense RNA genome and, together with Ebola virus (EBOV), constitutes the family *Filoviridae* (30). Since the first cases of MARV infection were documented in Germany and Yugoslavia in 1967, sporadic outbreaks of Marburg hemorrhagic fever have been reported, mainly in Central Africa (23). The case fatality rate of the largest outbreak in Angola in 2004 to 2005 reached 88%. Although MARVs were isolated from Egyptian fruit bats (*Rousettus aegyptiacus*) in Uganda (42), the transmission routes to humans and nonhuman primates and the mechanisms whereby MARVs are perpetuated in nature are not fully understood. Currently, there is neither effective prophylaxis nor treatment available for filovirus infection. Thus, together with Ebola virus, MARV poses a significant public health threat in Central Africa and is feared worldwide as a potentially imported infectious pathogen and a biothreat agent.

Filovirus particles consist of at least seven structural proteins, including the sole transmembrane glycoprotein (GP) on their surface. GP undergoes proteolytic cleavage by host proteases such as furin, resulting in two subunits, GP1 and GP2, which are linked by a disulfide bond (46). GP is highly glycosylated with large amounts of N- and O-linked glycans, most of which are located in its middle one-third, designated the mucin-like region (5, 6). The primary function of GP is as a mediator of virus entry into host cells (40, 50), and therefore, GP is believed to be the only target of neutralizing antibodies against filoviruses.

Previous studies that focused on the interaction between EBOV GP and neutralizing monoclonal antibodies (MAbs) indicated that the direct inhibition of GP attachment to its ligand(s)/receptor(s) or the fusion of viral and host cell membranes is likely to be a key mechanism of neutralization (17, 33, 38). Our most

recent study demonstrated that passive immunization with well-characterized neutralizing MAbs had beneficial effects in a non-human primate model of Ebola hemorrhagic fever (21), highlighting the potential of antibody therapy against filovirus infection. In contrast, little is known about MAbs that efficiently neutralize MARV infectivity *in vitro* and the mechanisms of the antibody-mediated inhibition of MARV infectivity, although passive prophylaxis with polyclonal IgG antibodies was shown previously to protect nonhuman primates from lethal MARV infection (4).

While virion structural protein 40 (VP40), the major viral matrix protein, is the key driving force for the budding of progeny virions (10, 11, 18, 27, 41), filovirus GPs are also known to be involved in the virus budding process. EBOV GP-expressing cells produce virosome-like structures possessing GP spikes on their surface, although these particles are pleomorphic and not similar morphologically to authentic virions (27). Furthermore, upon the coexpression of GP and VP40 in cultured cells, virus-like particles (VLPs) morphologically resembling authentic virions are efficiently released into culture media (27, 43). This outward machinery (i.e., virus budding), indispensable for viral replication and dissemination, might be another target of protective antibodies. It is known that nonneutralizing antibodies against influenza A vi-

Received 20 July 2012 Accepted 20 September 2012

Published ahead of print 3 October 2012

Address correspondence to Ayato Takada, atakada@czz.hokudai.ac.jp.

Supplemental material for this article may be found at <http://jvi.asm.org/>.

Copyright © 2012, American Society for Microbiology. All Rights Reserved.

doi:10.1128/JVI.01896-12

rus neuraminidase, which mediates the release of progeny viruses from host cells, play a role in protective immunity (12, 26, 48). It was also demonstrated *in vitro* that the particle release of some viruses (e.g., bovine leukemia, vaccinia, Sendai, and rubella viruses) from infected cells was reduced in the presence of MAbs or antiserum (1, 2, 28, 45).

In this study, we found that murine MAbs AGP127-8 and MGP72-17 remarkably reduced the extracellular release of MARV from infected cells, whereas these antibodies did not inhibit the GP-mediated entry of MARV into host cells. We further confirmed that AGP127-8 and MGP72-17 decreased the amount of VLPs produced by cells expressing GP, VP40, and nucleoprotein (NP) of MARV, suggesting that the MAbs inhibited the budding of progeny virions from infected cells. These findings were confirmed by morphological analyses that revealed that VLPs were densely bundled and accumulated on the surfaces of VLP-producing cells cultured in the presence of AGP127-8 and MGP72-17. Here we discuss a novel mechanism of the antibody-mediated inhibition of virus infectivity that differs from “classical” neutralization activity.

MATERIALS AND METHODS

Viruses and cells. MARV strain Angola (51) was propagated in Vero E6 cells (kindly provided by R. Baric, University of North Carolina, Chapel Hill, NC) and stored at -80°C until use. All infectious work with MARV was performed in biosafety level 4 laboratories at the Integrated Research Facility of the Rocky Mountain Laboratories, Division of Intramural Research, National Institute of Allergy and Infectious Diseases, National Institutes of Health, Hamilton, MT. Replication-incompetent vesicular stomatitis virus (VSV) pseudotyped with MARV (Angola) GP expressing green fluorescent protein was generated as described previously (40). A neutralizing MAb to the VSV G protein, VSV-G(N)1-9 (24), was used to abolish the background infectivity of parental VSV bearing the VSV G protein. The infectious units (IU) of VSV bearing MARV GP were determined by counting the number of Vero E6 cells expressing green fluorescent protein under a fluorescence microscope. Vero E6 and human embryonic kidney 293T (HEK293T) cells (3) were grown in Dulbecco's modified Eagle's medium. Mouse myeloma P3-U1 cells and hybridoma cell lines were maintained in RPMI 1640 medium. The media were supplemented with fetal calf serum and antibiotics.

Monoclonal antibodies. MARV GP-specific MAbs AGP2-1 (IgG1), AGP126-15 (IgG1), AGP127-8 (IgG1), AΔM16-2-13 (IgM), and MGP72-17 (IgM) were generated as described previously (24). Briefly, HEK293T cells were transfected with plasmids encoding MARV GP and VP40. VLPs produced and released into the supernatant were purified by ultracentrifugation through a 25% sucrose cushion. Five-week-old female BALB/c mice were immunized intramuscularly and subcutaneously with 150 μg of VLP 3 times at 3-week intervals. Three weeks after the last immunization, mice were boosted intraperitoneally with 150 μg of VLPs. Three days later, spleen cells from these mice were fused with P3-U1 cells and maintained according to a standard procedure (32). Hybridomas were screened for the secretion of MARV GP-specific MAbs by an enzyme-linked immunosorbent assay (ELISA), using purified C-terminally histidine-tagged MARV GP as an antigen (25), and hybridoma-producing MAbs were cloned by limiting dilution of the cells. The isotypes of the obtained MAbs were determined by using a mouse MAb isotyping test kit (AbD Serotec), according to the manufacturer's instructions. Protein A-agarose columns (Bio-Rad) and Kaptive-M (Tecnogen) were used to purify monoclonal IgG and IgM, respectively, from mouse ascites. H5-61-2-1 (IgG1) and APH159-1-3 (IgM), specific for influenza A virus hemagglutinins, were used as irrelevant control antibodies. AGP2-1 (IgG1), whose epitope is different from that of AGP127-8 (24), and MVP40 1-17-1, specific for MARV VP40, were conjugated with Alexa Fluor 488 and 647, respectively, by using Zenon mouse IgG1 labeling kits

(Invitrogen) for immunofluorescence analysis (see below). Animal studies were carried out in strict accordance with guidelines for proper conduct of animal experiments of the Science Council of Japan (31a). The protocol was approved by the Hokkaido University Animal Care and Use Committee. All efforts were made to minimize suffering.

Purification of AGP127-8 antigen-binding fragment (Fab). Purified AGP127-8 was digested by papain, and the Fab fractions were yielded through ion-exchange chromatography by using diethylethanolamine (Toyopearl DEAE-650 M; Tosoh Corporation). Following solvent displacement with 10 mM sodium phosphate (pH 6.8), the samples containing Fab were fractionated by gel filtration chromatography (TSKgel G3000SW; Tosoh Corporation), and the Fab fraction was subjected to solvent displacement with phosphate-buffered saline (PBS) and concentrated by ultrafiltration (molecular weight cutoff of 10,000 [10K]).

Detection of MARV particles and VLPs released into culture media. Vero E6 cells grown in 12-well plates were inoculated with MARV at a multiplicity of infection (MOI) of 1.0 and cultured at 37°C with medium containing 50, 10, or 2 $\mu\text{g}/\text{ml}$ of MAbs or in the absence of MAbs. At 24, 48, 72, and 96 h postinoculation (hpi), supernatants were harvested and cleared of cell debris. Samples were analyzed directly by sodium dodecyl sulfate-polyacrylamide gel electrophoresis (SDS-PAGE) and Western blotting. For VLP assays, HEK293T cells grown in 24-well plates were cotransfected with mammalian expression plasmid pCAGGS encoding MARV GP (pC-AngolaGP), VP40 (pC-AngolaVP40), and NP (pC-AngolaNP) and maintained in medium containing 50, 10, or 2 $\mu\text{g}/\text{ml}$ of the respective MAbs or the AGP127-8 Fab. At 48 h posttransfection, supernatants were collected and cleared from cell debris. Pellets and cells were treated with lysis buffer (0.1 M Tris-HCl [pH 7.5], 0.1 M NaCl, 1% Nonidet P-40, 1% Triton X-100, and Complete miniprotease inhibitor [Roche]) and centrifuged to remove insoluble fractions. Supernatants and cell lysates were subjected to SDS-PAGE and Western blotting.

Neutralization tests. Serial dilutions of MAbs were prepared in Dulbecco's modified Eagle's medium supplemented with 2% fetal bovine serum, and 25 μl was incubated with 200 focus-forming units of MARV in a total volume of 50 μl . After 30 min at 37°C , the MAB-virus mixture was used to inoculate Vero E6 cells seeded into a 48-well plate, and cells were incubated for 60 min at 37°C . Next, the mixture was removed from the cells, and 0.5 ml of a 1.2% carboxymethyl cellulose–minimum essential medium (MEM) (Life Technologies) solution was added to each well. Following incubation for 4 days at 37°C , the plates were fixed with 10% neutral buffered formalin. Subsequently, the cells were permeabilized, and foci were stained with anti-MARV NP rabbit serum produced by immunization with a synthetic peptide corresponding to amino acid residues 591 to 605 (GDILEPIRSPSSPSA) of MARV strain Angola, designated FS0609, followed by a fluorescein isothiocyanate-labeled secondary antibody (Sigma), as described previously (21). Foci were counted by using a fluorescence microscope. The neutralization test for pseudotyped VSV was done as described previously (37). Briefly, VSVs pseudotyped with MARV GP ($10^{4.5}$ IU/ml) were mixed with each appropriately diluted MAb, incubated for 1 h at room temperature, and inoculated into confluent Vero E6 cells grown in 96-well plates. At 18 hpi, infectivity was determined by counting fluorescent cells. The relative percentage of infectivity was calculated by setting the number of cells infected in the absence of GP-specific MAbs to 100%.

SDS-PAGE and Western blotting. Samples were analyzed by 7.5% SDS-PAGE and Western blotting, as mentioned elsewhere previously (25). Briefly, cell culture supernatants or cell lysates were mixed with SDS-PAGE sample buffer with 5% 2-mercaptoethanol and heated for 5 min at 98°C . After electrophoresis, separated proteins were blotted onto a polyvinylidene difluoride membrane (Millipore). FS0609 and a mouse monoclonal anti- β -actin antibody (AC-15; Abcam) were used as primary antibodies to detect MARV NP and β -actin, respectively. The bound antibodies were detected with peroxidase-conjugated AffiniPure donkey anti-rabbit IgG(H+L) (Jackson ImmunoResearch) and goat anti-mouse

IgG(H+L) (Jackson ImmunoResearch), followed by visualization with Immobilon Western (Millipore).

ELISA. A filovirus GP-based ELISA was performed as described previously (25). Briefly, ELISA plates (Nunc Maxisorp) were coated with purified soluble MARV GP lacking the transmembrane domain (100 ng/50 μ l/well), followed by blocking with 3% skim milk (200 μ l/well). Appropriately diluted cultured media of hybridomas or purified MABs were prepared, added to the ELISA plates, and incubated for 1 h at room temperature. Bound antibodies were visualized by adding secondary peroxidase-conjugated goat anti-mouse IgG and 3,3',5,5'-tetramethylbenzidine (Sigma). The reaction was stopped by the addition of 1 N sulfuric acid to the mixture, and the optical density at 450 nm was measured.

Immunofluorescence microscopy. HEK293T cells grown on a glass chamber slide were transfected with pC-AngolaGP, pC-AngolaVP40, and pC-AngolaNP or an equivalent quantity of an empty vector (pCAGGS) and maintained in the presence (50 μ g/ml) or absence of MABs. At 24 h posttransfection, cells were fixed with 4% paraformaldehyde for 30 min. Following the removal of the fixative, the remaining aldehydes were quenched with 100 mM glycine in PBS. After washing with PBS, cells were permeabilized with 0.1% Triton X-100 in PBS and incubated in blocking solution (2% bovine serum albumin, 0.2% Tween 20, 5% glycerol, and 0.05% sodium azide in PBS). GP and VP40 were stained with AGP2-1 conjugated with Alexa Fluor 488 and MVP40 1-17-1 conjugated with Alexa Fluor 647, respectively. NP was detected with F50609 and goat anti-rabbit IgG conjugated with Alexa Fluor 405 (Invitrogen). After staining, samples were fixed with 4% paraformaldehyde for 15 min. Fluorescent images were acquired by using an LSM 780 microscope (Zeiss).

Electron microscopy. Transmission electron microscopy (TEM) and scanning electron microscopy (SEM) were carried out as described previously (27, 47). For ultrathin sections, 48 h after the transfection of HEK293T cells with pC-AngolaGP and pC-AngolaVP40, the cells were fixed for 20 min with 2.5% glutaraldehyde in 0.1 M cacodylate buffer (pH 7.4). Cells were scraped off the 12-well plate, pelleted by low-speed centrifugation, and then fixed for 30 min with the same fixative. Small pieces of the fixed pellet were washed with cacodylate buffer, postfixed with 2% osmium tetroxide in cacodylate buffer for 1 h at 4°C, dehydrated with a series of ethanol gradients followed by propylene oxide, embedded in an Epon 812 resin mixture (TAAB Laboratories Equipment Ltd.), and polymerized at 60°C for 2 days. Thin sections were stained with uranyl acetate and lead citrate and examined with a Tecnai F20 electron microscope at 200 kV. For SEM, HEK293 cells transfected with pC-AngolaGP and pC-AngolaVP40 were fixed at 48 h posttransfection. The fixed cells were dehydrated with a series of ethanol gradients, substituted with *t*-butanol, and dried in a Hitachi ES-2030 freeze-dryer. Dried specimens were coated with osmium tetroxide by using an HPC-1S osmium coater (Vacuum Device Inc.) and examined with a Hitachi S-4200 microscope.

RESULTS

MARV GP-specific MABs that inhibit virus release from infected cells. In a virus-neutralizing test, infectious viruses are generally mixed with antibodies prior to inoculation onto cultured cells, and the reduction of infectivity is estimated by plaque counts or cytopathic effects. However, in the assay applied here, MARV was first inoculated onto Vero E6 cells at an MOI of 1 without preincubation with MABs and then cultured in the media containing MABs. The amounts of virus particles released into the culture supernatants were estimated by detecting virion-associated NP by Western blotting. This assay enabled us to evaluate the abilities of MABs to inhibit the production of virus particles from infected cells in a single replication cycle of MARV infection. We tested 4 murine MARV GP-specific MABs, AGP126-15 (IgG1), AGP127-8 (IgG1), A Δ M16-2-13 (IgM), and MGP72-17 (IgM), in regard to their inhibitory activities against MARV particle production (Fig. 1).

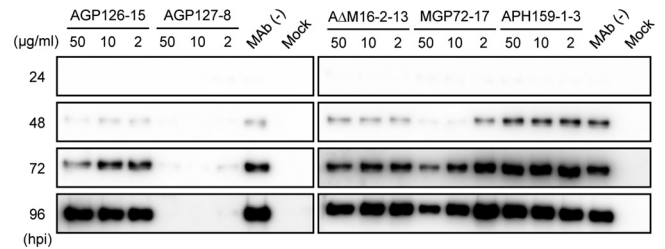


FIG 1 Detection of NP in the supernatants of cells infected with MARV. Vero E6 cells were infected with MARV at an MOI of 1.0. Following a 1-h incubation for virus adsorption, cells were cultured in media containing 50, 10, or 2 μ g/ml of GP-specific IgG (AGP126-15 and AGP127-8) or IgM (A Δ M16-2-13 and MGP72-17) or an irrelevant negative-control MAB (APH159-1-3) or without MABs. Supernatants were collected every 24 hpi over 96 hpi. NP in the virus particles released into the supernatants was detected by Western blotting, as described in Materials and Methods. Experiments were conducted three times, and representative data are shown.

In the absence of MABs, NP was detected in the culture supernatants at 48 hpi, and the NP signal was increased in a time-dependent manner, indicating increased virus release from infected cells over time. Similarly, NP was detected in the supernatants of cells maintained in the presence of a negative-control MAB, APH159-1-3. AGP126-15 and A Δ M16-2-13 only slightly reduced the amount of NP in the supernatants. In contrast, AGP127-8 and MGP72-17 showed remarkable inhibitory effects on virus release. In the presence of 10 or 50 μ g/ml of MGP72-17, NP was almost undetectable in the supernatant collected at 48 hpi, and the intensity of the NP bands was obviously lower than that of the bands seen in the presence of the control MAB up to 96 hpi. Most surprisingly, NP was hardly detected over 96 hpi in the presence of AGP127-8, even at the lowest concentration tested (2 μ g/ml).

Absence of neutralizing activity of MABs AGP127-8 and MGP72-17. To clarify whether these antibodies have overlapping potential with neutralizing activity that blocks virus entry into host cells, the MABs were assessed with a traditional neutralization test using VSV pseudotyped with MARV GP (Fig. 2A and B). We found that neither of the GP-specific IgG MABs (AGP126-15 and AGP127-8) tested showed neutralizing activity, although the IgM MABs (A Δ M16-2-13 and MGP72-17) showed minimal neutralizing activity at high concentrations (Fig. 2B). Similarly, the infectivity of authentic MARV was not reduced by these MABs in the neutralization test (Fig. 2C). Importantly, AGP127-8, which almost completely inhibited MARV release from infected cells (Fig. 1), showed no neutralizing activity. Taken together, these results indicate that the “classical” neutralizing activity of MABs is not required to inhibit the extracellular release of virus particles.

Inhibition of VLP formation by AGP127-8 and MGP72-17. Since AGP127-8 and MGP72-17, which do not block the GP-mediated entry of MARV into host cells, drastically reduced the release of progeny viruses, we assumed that AGP127-8 and MGP72-17 inhibit virus budding. To directly verify this hypothesis, we utilized a simple VLP formation assay. HEK293T cells were cotransfected with mammalian expression plasmid pCAGGS encoding MARV GP, VP40, and NP, and the amounts of NP incorporated into extracellular VLPs or accumulated in cells were estimated by Western blotting (Fig. 3). Consistent with the results shown in Fig. 1, AGP127-8 and MGP72-17 significantly reduced VLP formation in a dose-dependent manner, whereas AGP126-15

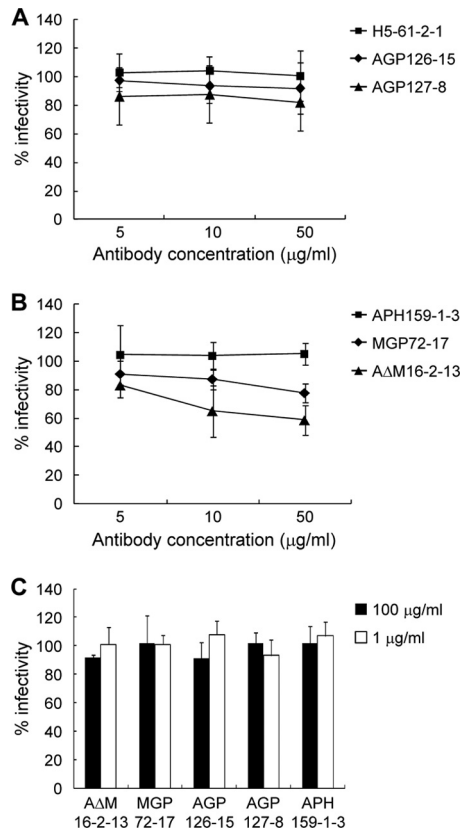


FIG 2 Neutralizing activity of MABs. (A and B) VSV pseudotyped with MARV GP was incubated with 5, 10, or 50 µg/ml of GP-specific IgG (A) or IgM (B) MABs for 1 h and subsequently inoculated into confluent Vero E6 cells. (C) Neutralizing activities of MABs were also tested for authentic MARV. H5-61-2-1 and APH159-1-3 were used as irrelevant negative-control MABs. Experiments using pseudotyped VSV (A and B) and MARV (C) were performed 3 and 2 times, respectively, and averages and standard deviations are shown.

and AΔM16-2-13 did not remarkably alter the amounts of NP detected in the supernatants compared to control MABs H5-61-2-1 and APH159-1-3 (Fig. 3A and B). Interestingly, the NP amounts were increased reciprocally in the lysates of VLP-producing cells incubated in the presence of AGP127-8 or MGP72-17, suggesting the cellular accumulation of NP due to the decreased extracellular VLP release. AGP127-8 exhibited the highest level of activity of budding inhibition among the tested MABs. The VLP release of another MARV strain (Musoke) was also reduced by AGP127-8 and MGP72-17 (data not shown). Neither AGP127-8 nor MGP72-17 inhibited the budding of VLPs composed of MARV VP40 and NP (data not shown). Taken together, these data suggest that AGP127-8 and MGP72-17 inhibit VLP egress from cells, most likely by interfering with the budding process mediated by VP40 and GP.

To evaluate whether the multivalent binding of the IgG variable regions is of significance in regard to the capacity to inhibit budding, the potential of the AGP127-8 Fab was assessed in comparison to that of intact AGP127-8 IgG (Fig. 3C). Interestingly, the amount of NP detected in the presence of the AGP127-8 Fab was comparable to that in the control supernatant (i.e., without MAB), and NP accumulation was not observed in the cells. These results indicate that the bivalency of IgG binding to multiple GP molecules is essential for the inhibition of VLP formation.

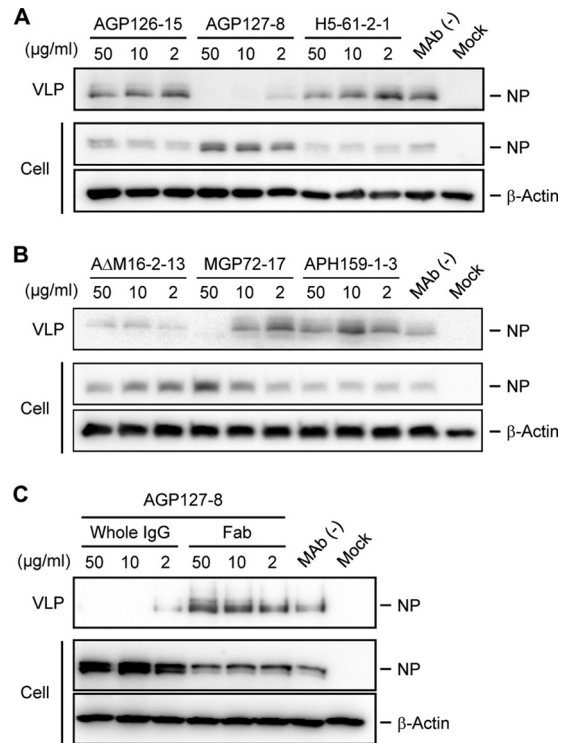


FIG 3 Detection of VLPs in the supernatants of cells expressing GP, VP40, and NP. (A and B) Subconfluent HEK293T cells were cotransfected with pC-AngolaGP, pC-AngolaVP40, and pC-AngolaNP or the empty vector pCAGGS (mock) and maintained with 50, 10, or 2 µg/ml of MABs or without MABs. At 48 h posttransfection, supernatants and cell lysates were subjected to SDS-PAGE, followed by Western blotting. (C) The AGP127-8 Fab was also tested under the same conditions. Experiments were conducted three times, and a representative data set is shown.

Localization of GP, VP40, and NP in VLP-producing cells. To further investigate the mechanisms by which AGP127-8 and MGP72-17 reduce budding efficiency, HEK293T cells transfected with GP-, VP40-, and NP-expressing plasmids were cultured with or without these MABs and examined by confocal microscopy (Fig. 4). The distributions of GP, VP40, and NP in the cells were separately visualized by multiple staining with Alexa Fluor. In the absence of MABs, numerous filamentous structures accompanied by GP, VP40, and NP, some of which were most likely filopodia (15), protruded from the cell surface. Similar filamentous structures were observed for cells treated with control MABs AGP126-15 and AΔM16-2-13, although the filamentous protrusions were slightly shortened (Fig. 4). In contrast, when transfected cells were cultured in the presence of AGP127-8 or MGP72-17, these viral proteins were colocalized but accumulated mainly along smooth cell surfaces, with few protruding filamentous structures. Since the overall expression levels and distributions of GP, VP40, and NP in the cells did not seem to be altered by AGP127-8 and MGP72-17, the diminished elongation of filamentous structures might be associated with impaired VLP release in the presence of these MABs.

We then examined the distribution of AGP127-8 itself in HEK293T cells expressing GP, VP40, and NP, since the uptake of virus-specific antibodies bound to viral proteins expressed on the cells was reported previously for human cytomegalovirus-infected

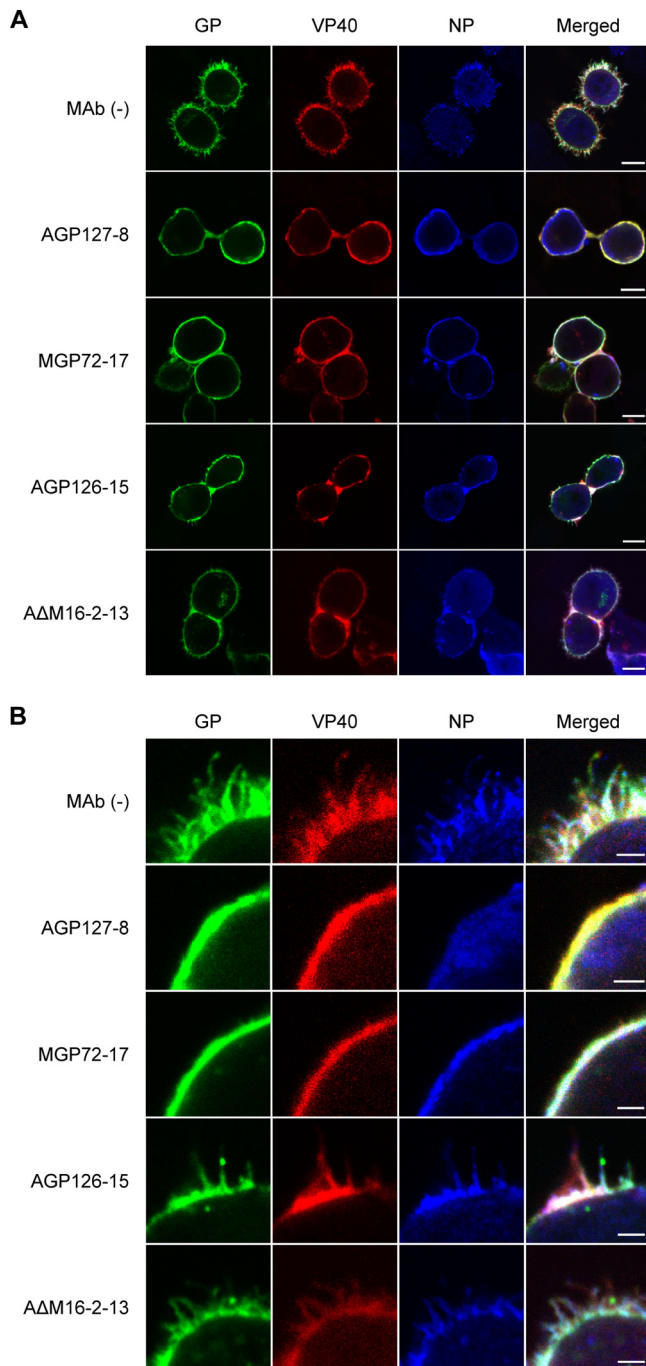


FIG 4 Immunofluorescence images of cells expressing GP, VP40, and NP in the presence of antibodies. HEK293T cells transfected with pC-AngolaGP, pC-AngolaVP40, and pC-AngolaNP were incubated in the absence or presence of the respective antibodies. GP and VP40 were probed by using AGP2-1 conjugated with Alexa Fluor 488 and MVP40 1-17-1 conjugated with Alexa Fluor 647, respectively. NP was detected with the anti-NP rabbit serum FS0609 and goat anti-rabbit IgG antibody conjugated with Alexa Fluor 405. Low (A)- and high (B)-magnification images are shown, with scale bars of 10 μm (A) and 2 μm (B).

cells (20), and therefore, it might be possible that AGP127-8 bound to GP was introduced into cells and negatively affected VLP formation intracellularly. However, AGP127-8 was detected only on the surfaces of cells expressing GP, VP40, and NP (see Fig. S1 in

the supplemental material), indicating that AGP127-8 inhibited VLP formation extracellularly.

Determination of cell surface morphology of VLP-producing cells by electron microscopy. To gain insight into the mechanism of the antibody-mediated inhibitory effects on the MARV budding process, we examined HEK293T cells expressing GP and VP40 using TEM and SEM. We found that cells cultured without MABs produced filamentous VLPs budding from the cell surface (Fig. 5A, D, and G), as reported previously (27). In the absence of MABs, numerous filamentous prominences were observed on the cell surface (Fig. 5D and G), consistent with the immunocytochemical analyses shown in Fig. 4. A similar VLP formation was found for cells treated with control MAB $\Delta\Delta\text{M16-2-13}$ or AGP126-15 (see Fig. S3 in the supplemental material). In contrast, VLPs were not released efficiently from cells in the presence of AGP127-8 and MGP72-17 (Fig. 5B and C) and appeared to be tangled and piled up on the cell surface (Fig. 5E, F, H, and I). The abnormal accumulation of filamentous structures, most likely unformed VLPs that were not pinched off from the cell membrane, was also found in ultrathin sections of the cells cultured with AGP127-8 or MGP72-17 (Fig. 5B and C). These data suggest that AGP127-8 and MGP72-17 bundle filamentous VLPs on the cell surface during the budding process (Fig. 5E, F, H, and I).

DISCUSSION

In general, neutralizing antibodies recognize epitopes on viral surface proteins and block essential steps for the invasion of viruses into host cells, such as attachment to viral receptors and the fusion of the viral envelope with the plasma membrane. Several MABs to EBOV GP, for example, KZ52, ZGP133/3.16, and JP3K11, were shown to neutralize EBOV effectively *in vitro* by inhibiting the cellular entry pathway of the virus (16, 17, 33, 37, 38). In contrast, there has been no report demonstrating an effective neutralizing MAB against MARV. However, it was recently shown that the passive immunization of nonhuman primates with antibodies was fully protective against lethal MARV and EBOV infection (4, 29), suggesting the pivotal role of antibodies in protective immunity. In the present study, we propose a novel mechanism by which antibodies counteract MARV particle budding.

We found that the budding and extracellular release of MARV were inhibited by MABs AGP127-8 and MGP72-17 (Fig. 1), whereas these MABs did not display “classical” neutralizing activity (Fig. 2). Morphological analyses by electron microscopy suggested that AGP127-8 and MGP72-17 deposited a tremendous number of unreleased VLPs on the cell surface (Fig. 5). On the other hand, the AGP127-8 Fab did not inhibit VLP budding (Fig. 3C), indicating that multiple antigen-binding sites of the intact IgG are a prerequisite for budding inhibition. Thus, the most plausible explanation for the mechanism underlying the inhibitory effects of these GP-specific MABs on virus particle budding is that the antibodies cross-link multiple GP molecules expressed on the infected-cell surface before the initiation of the budding process, and consequently, this intricate cross-linkage via antibodies and GPs mechanically interferes with the driving force for MARV budding, resulting in the accumulation of premature and unreleased virus particles on the cells.

It might also be possible that the interaction between antibodies and cell surface GPs causes intracellular signaling against viral protein transport and/or assembly. It was shown previously that VP40 is the key factor for filovirus assembly and budding, which

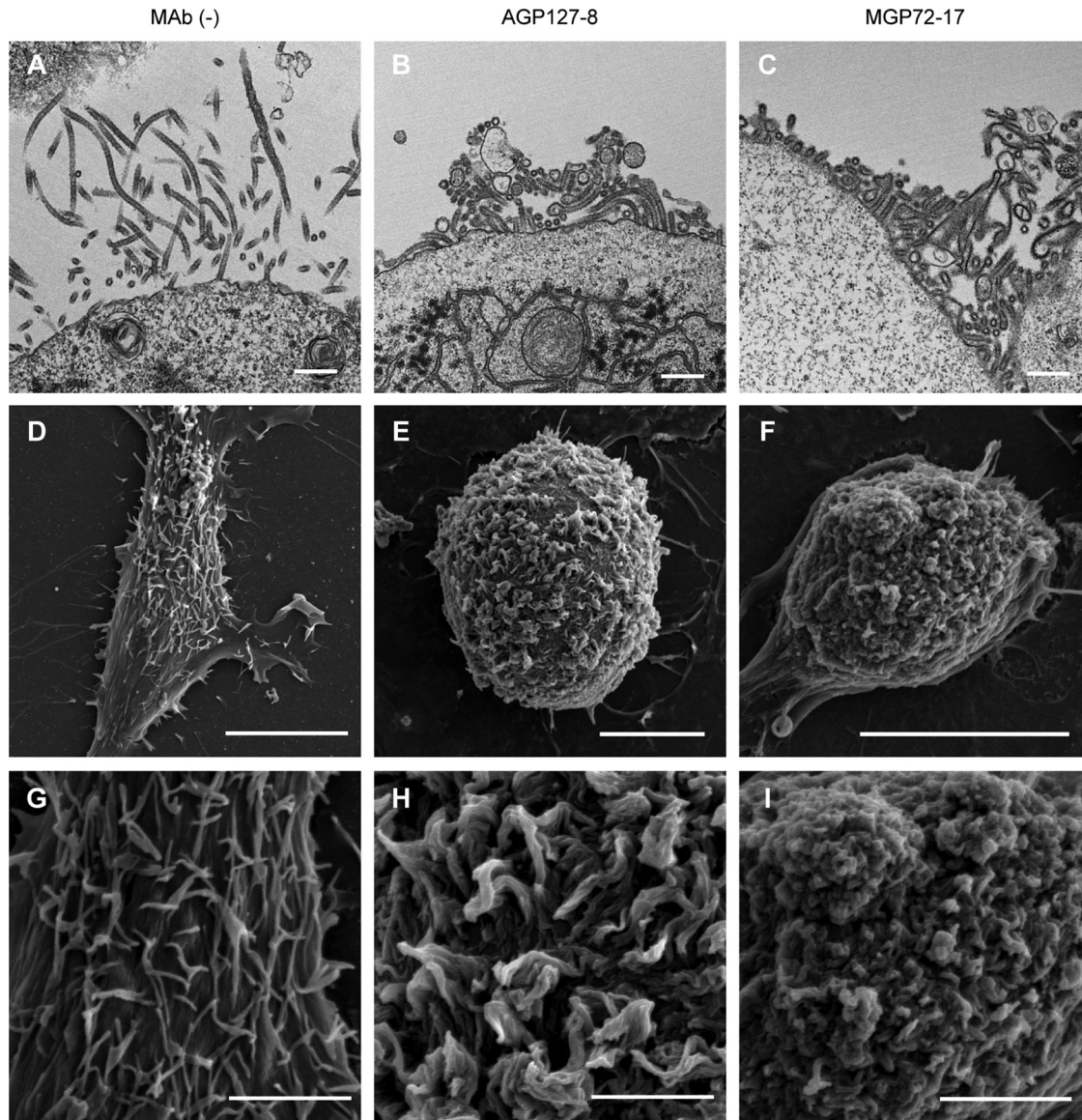


FIG 5 TEM and SEM images of cells expressing GP and VP40 in the presence of AGP127-8 or MGP72-17. HEK293T cells transfected with pC-AngolaGP and pC-AngolaVP40 were incubated in the absence (A, D, and G) or presence of either AGP127-8 (B, E, and H) or MGP72-17 (C, F, and I). (A to C) Ultrathin sections were examined by TEM. (D to I) SEM images are shown at low (D to F) and high (G to I) magnifications. Scale bars represent 500 nm (A to C), 10 μ m (D to F), and 3 μ m (G to I).

require its interaction with host proteins (19). The majority of MARV VP40 is transported to the cell surface along with GP through a retrograde endosomal pathway by hijacking the ESCRT machinery of the cells, and newly assembled virions are finally released from host cells (9, 13, 14, 43, 44). Thus, such cellular machinery utilized for the assembly and budding of MARV might be affected by intracellular signaling via the interaction between GP-specific antibodies and GPs on the cell surface. There are indeed several examples of such a phenomenon (e.g., varicella-zoster or measles virus infection), in which the binding of virus-specific antibodies to viral proteins expressed on the cell surface suppressively modulates the distribution and synthesis patterns of viral proteins in infected cells (7, 8, 31, 34, 52).

Interestingly, the inhibition of MARV budding by AGP127-8

was not simply dependent on its affinity for GP, since AGP127-8 and AGP126-15 showed similar capacities for binding to GPs (see Fig. S3 in the supplemental material), whereas a remarkable difference in the budding inhibition activities was seen between these MAbs. This indicates that the epitopes of these MAbs are likely the critical factor for the inhibitory activity. Both AGP127-8 and AGP126-15 recognize epitopes (amino acid positions 411 to 430 and 369 to 385, respectively) located in the mucin-like region of GP (24). The mucin-like region plays an important role in attachment to the preferred target cells (e.g., hepatocytes, endothelial cells, dendritic cells, and macrophages), whose infection is likely involved in filovirus pathogenesis (36). Importantly, however, the mucin-like region is not essential for the fundamental function of GP in viral entry into cells *in vitro* (22, 35, 39) and thus is unlikely

to contain important epitopes for neutralizing antibodies. On the other hand, our data suggest that some antibodies recognizing epitopes on the mucin-like region, such as AGP127-8, have strong activity to inhibit MARV budding, which leads to the reduced production of progeny viruses. Note that the epitope of AGP127-8 is located near the furin cleavage site at the C terminus of GP1, which is likely unexposed on the uncleaved GP molecules (see Fig. S4 in the supplemental material). Thus, it can be hypothesized that the C terminus of cleaved GP1 might have some biological functions to facilitate extracellular virus release.

The present study proposes a novel mechanism of the antibody-mediated inhibition of MARV infection. It would be of interest to investigate whether certain EBOV GP-specific MABs also have a similar capacity to inhibit the process of virus budding. It should be noted that passively transferred anti-EBOV GP non-neutralizing MABs recognizing epitopes in the mucin-like region were protective in a mouse model of lethal EBOV infection (49). As evidenced by the well-known efficacy of influenza virus neuraminidase inhibitors, the viral budding process is a promising target for antiviral development. Our data lead to the idea that “classical” neutralizing activity is not the only indicator of protective antibody and that MABs like AGP127-8 may have the potential for prophylactic and therapeutic use. Recent reports demonstrated that antibody therapy is a promising strategy for the treatment of filovirus infection (4, 21, 29). Furthermore, a detailed analysis of the precise mechanism by which MABs interfere with the virus budding process may provide new insights into the development of prophylactic and therapeutic measures against virus infections.

ACKNOWLEDGMENTS

We thank Hiroko Miyamoto, Ayaka Yokoyama, Kazumasa Yokoyama, Manabu Igarashi (Hokkaido University Research Center for Zoonosis Control), and Hideki Ebihara (National Institute of Allergy and Infectious Diseases, National Institutes of Health, Rocky Mountain Laboratories) for technical assistance or valuable advice and Kim Barrymore for editing the manuscript.

This work was supported by the Japan Initiative for Global Research Network on Infectious Diseases (J-GRID); the Global COE Program; a grant-in-aid from the Ministry of Education, Culture, Sports, Science and Technology (MEXT); ERATO (Japan Science and Technology Agency); and National Institute of Allergy and Infectious Disease Public Health Service research grants. Funding was also provided by a grant-in-aid from the Ministry of Health, Labour and Welfare of Japan and by the Division of Intramural Research, National Institute of Allergy and Infectious Diseases, National Institutes of Health.

REFERENCES

1. Corboba P, Grutaduria S, Cuffini C, Zapata M. 2000. Neutralizing monoclonal antibody to the E1 glycoprotein epitope of rubella virus mediates virus arrest in VERO cells. *Viral Immunol.* 13:83–92.
2. Driscoll DM, Onuma M, Olson C. 1977. Inhibition of bovine leukemia virus release by antiviral antibodies. *Arch. Virol.* 55:139–144.
3. DuBridge RB, et al. 1987. Analysis of mutation in human cells by using an Epstein-Barr virus shuttle system. *Mol. Cell. Biol.* 7:379–387.
4. Dye JM, et al. 2012. Postexposure antibody prophylaxis protects nonhuman primates from filovirus disease. *Proc. Natl. Acad. Sci. U. S. A.* 109:5034–5039.
5. Feldmann H, Nichol ST, Klenk HD, Peters CJ, Sanchez A. 1994. Characterization of filoviruses based on differences in structure and antigenicity of the virion glycoprotein. *Virology* 199:469–473.
6. Feldmann H, Will C, Schikore M, Slenczka W, Klenk HD. 1991. Glycosylation and oligomerization of the spike protein of Marburg virus. *Virology* 182:353–356.
7. Fujinami RS, Norrby E, Oldstone MB. 1984. Antigenic modulation induced by monoclonal antibodies: antibodies to measles virus hemagglutinin alters expression of other viral polypeptides in infected cells. *J. Immunol.* 132:2618–2621.
8. Fujinami RS, Oldstone MB. 1980. Alterations in expression of measles virus polypeptides by antibody: molecular events in antibody-induced antigenic modulation. *J. Immunol.* 125:78–85.
9. Harty RN. 2009. No exit: targeting the budding process to inhibit filovirus replication. *Antiviral Res.* 81:189–197.
10. Harty RN, Brown ME, Wang G, Huibregtse J, Hayes FP. 2000. A PPxY motif within the VP40 protein of Ebola virus interacts physically and functionally with a ubiquitin ligase: implications for filovirus budding. *Proc. Natl. Acad. Sci. U. S. A.* 97:13871–13876.
11. Jasenosky LD, Neumann G, Lukashevich I, Kawaoka Y. 2001. Ebola virus VP40-induced particle formation and association with the lipid bilayer. *J. Virol.* 75:5205–5214.
12. Johansson BE, Grajower B, Kilbourne ED. 1993. Infection-permissive immunization with influenza virus neuraminidase prevents weight loss in infected mice. *Vaccine* 11:1037–1039.
13. Kolesnikova L, Bamberg S, Berghöfer B, Becker S. 2004. The matrix protein of Marburg virus is transported to the plasma membrane along cellular membranes: exploiting the retrograde late endosomal pathway. *J. Virol.* 78:2382–2393.
14. Kolesnikova L, Berghöfer B, Bamberg S, Becker S. 2004. Multivesicular bodies as a platform for formation of the Marburg virus envelope. *J. Virol.* 78:12277–12287.
15. Kolesnikova L, Bohil AB, Cheney RE, Becker S. 2007. Budding of Marburgvirus is associated with filopodia. *Cell. Microbiol.* 9:939–951.
16. Lee JE, et al. 2008. Structure of the Ebola virus glycoprotein bound to a human survivor antibody. *Nature* 454:177–182.
17. Lee JE, Saphire EO. 2009. Neutralizing ebolavirus: structural insights into the envelope glycoprotein and antibodies targeted against it. *Curr. Opin. Struct. Biol.* 19:408–417.
18. Licata JM, Johnson RF, Han Z, Harty RN. 2004. Contribution of Ebola virus glycoprotein, nucleoprotein, and VP24 to budding of VP40 virus-like particles. *J. Virol.* 78:7344–7351.
19. Liu Y, Harty RN. 2010. Viral and host proteins that modulate filovirus budding. *Future Virol.* 5:481–491.
20. Manley K, et al. 2011. Human cytomegalovirus escapes a naturally occurring neutralizing antibody by incorporating it into assembling virions. *Cell Host Microbe* 10:197–209.
21. Marzi A, et al. 2012. Protective efficacy of neutralizing monoclonal antibodies in a nonhuman primate model of Ebola hemorrhagic fever. *PLoS One* 7:e36192. doi:10.1371/journal.pone.0036192.
22. Matsuno K, et al. 2010. Different potential of C-type lectin-mediated entry between Marburg virus strains. *J. Virol.* 84:5140–5147.
23. Nakayama E, Takada A. 2011. Ebola and Marburg viruses. *J. Disaster Res.* 6:381–389.
24. Nakayama E, et al. 2011. Antibody-dependent enhancement of Marburg virus infection. *J. Infect. Dis.* 204:S978–S985. doi:10.1093/infdis/jir334.
25. Nakayama E, et al. 2010. Enzyme-linked immunosorbent assay for detection of filovirus species-specific antibodies. *Clin. Vaccine Immunol.* 17:1723–1728.
26. Nayak B, et al. 2010. Contributions of the avian influenza virus HA, NA, and M2 surface proteins to the induction of neutralizing antibodies and protective immunity. *J. Virol.* 84:2408–2420.
27. Noda T, et al. 2002. Ebola virus VP40 drives the formation of virus-like filamentous particles along with GP. *J. Virol.* 76:4855–4865.
28. Orvell C, Kristensson K. 1985. The effects of monoclonal antibodies against the hemagglutinin-neuraminidase and fusion protein on the release of Sendai virus from infected cells. *Arch. Virol.* 86:1–15.
29. Qiu X, et al. 2012. Successful treatment of Ebola virus-infected cynomolgus macaques with monoclonal antibodies. *Sci. Transl. Med.* 4:138ra81. doi:10.1126/scitranslmed.3003876.
30. Sanchez A, Geisbert TW, Feldmann H. 2007. Filoviridae: Marburg and Ebola viruses, p 1409–1448. In Knipe DM, et al (ed), *Fields virology*, 5th ed, vol 1. Lippincott Williams & Wilkins, Philadelphia, PA.
31. Schneider-Schaulies S, et al. 1992. Antibody-dependent transcriptional regulation of measles virus in persistently infected neural cells. *J. Virol.* 66:5534–5541.
- 31a. Science Council of Japan. 2006. Guidelines for proper conduct of animal experiments. <http://www.scj.go.jp/ja/info/kohyo/pdf/kohyo-20-k16-2e.pdf>.

32. Shahhosseini S, et al. 2007. Production and characterization of monoclonal antibodies against different epitopes of Ebola virus antigens. *J. Virol. Methods* **143**:29–37.
33. Shedlock DJ, et al. 2010. Antibody-mediated neutralization of Ebola virus can occur by two distinct mechanisms. *Virology* **401**:228–235.
34. Shiraki K, et al. 2011. Neutralizing anti-gH antibody of varicella-zoster virus modulates distribution of gH and induces gene regulation, mimicking latency. *J. Virol.* **85**:8172–8180.
35. Simmons G, Wool-Lewis RJ, Baribaud F, Netter RC, Bates P. 2002. Ebola virus glycoproteins induce global surface protein down-modulation and loss of cell adherence. *J. Virol.* **76**:2518–2528.
36. Takada A. 2012. Filovirus tropism: cellular molecules for viral entry. *Front. Microbiol.* **3**:34. doi:10.3389/fmicb.2012.00034.
37. Takada A, Ebihara H, Jones S, Feldmann H, Kawaoka Y. 2007. Protective efficacy of neutralizing antibodies against Ebola virus infection. *Vaccine* **25**:993–999.
38. Takada A, et al. 2003. Identification of protective epitopes on Ebola virus glycoprotein at the single amino acid level by using recombinant vesicular stomatitis viruses. *J. Virol.* **77**:1069–1074.
39. Takada A, et al. 2004. Human macrophage C-type lectin specific for galactose and N-acetylgalactosamine promotes filovirus entry. *J. Virol.* **78**:2943–2947.
40. Takada A, et al. 1997. A system for functional analysis of Ebola virus glycoprotein. *Proc. Natl. Acad. Sci. U. S. A.* **94**:14764–14769.
41. Timmins J, Scianimanico S, Schoehn G, Weissenhorn W. 2001. Vesicular release of Ebola virus matrix protein VP40. *Virology* **283**:1–6.
42. Towner JS, et al. 2009. Isolation of genetically diverse Marburg viruses from Egyptian fruit bats. *PLoS Pathog.* **5**:e1000536. doi:10.1371/journal.ppat.1000536.
43. Urata S, et al. 2007. Interaction of Tsg101 with Marburg virus VP40 depends on the PPPY motif, but not the PT/SAP motif as in the case of Ebola virus, and Tsg101 plays a critical role in the budding of Marburg virus-like particles induced by VP40, NP, and GP. *J. Virol.* **81**:4895–4899.
44. Urata S, Yasuda J. 2010. Regulation of Marburg virus (MARV) budding by Nedd4.1: a different WW domain of Nedd4.1 is critical for binding to MARV and Ebola virus VP40. *J. Gen. Virol.* **91**:228–234.
45. Vanderplasschen A, Hollinshead M, Smith GL. 1997. Antibodies against vaccinia virus do not neutralize extracellular enveloped virus but prevent virus release from infected cells and comet formation. *J. Gen. Virol.* **78**:2041–2048.
46. Volchkov VE, et al. 2000. Proteolytic processing of Marburg virus glycoprotein. *Virology* **268**:1–6.
47. Watanabe S, et al. 2004. Production of novel Ebola virus-like particles from cDNAs: an alternative to Ebola virus generation by reverse genetics. *J. Virol.* **78**:999–1005.
48. Webster RG, Reay PA, Laver WG. 1988. Protection against lethal influenza with neuraminidase. *Virology* **164**:230–237.
49. Wilson JA, et al. 2000. Epitopes involved in antibody-mediated protection from Ebola virus. *Science* **287**:1664–1666.
50. Wool-Lewis RJ, Bates P. 1998. Characterization of Ebola virus entry by using pseudotyped viruses: identification of receptor-deficient cell lines. *J. Virol.* **72**:3155–3160.
51. World Health Organization. 2005. Marburg haemorrhagic fever, Angola. *Wkly. Epidemiol. Rec.* **80**:158–159.
52. Zinnheimer-Dreikorn J, Koschel KP. 1990. Antigenic modulation of measles subacute sclerosing panencephalitis virus in a persistently infected rat glioma cell line by monoclonal anti-haemagglutinin antibodies. *J. Gen. Virol.* **71**:1391–1394.